Thermal Solid State Polymerization of *p*-Ethynylbenzoic Acid

Jeffrey M. Njus and Daniel J. Sandman*

Center for Advanced Materials, Department of Chemistry, University of Massachusetts Lowell, Lowell, Massachusetts 01854-5046

Lin Yang and Bruce M. Foxman*

Department of Chemistry, MS015, Brandeis University, Waltham, Massachusetts 02454-9110

Received April 20, 2005; Revised Manuscript Received July 13, 2005

ABSTRACT: While *p*-ethynylbenzoic acid (EBA) has been suggested to be reactive in the solid state, the structure−reactivity relationships and the nature of the product(s) have remained unknown. Crystallized from toluene, EBA is a monoclinic crystal, space group $P2_1/n$, $a = 3.8684(4)$, $b = 6.2329(4)$, $c = 30.190(3)$ Å; $\beta = 90.281(8)°$; $V = 727.90$ Å^3. The crystal structure contains linear chains and short intermolecular contacts between acetylene moieties, which provide a structural basis for initiation of topochemical reactivity. Heating of EBA leads to an amorphous poly(phenylacetylene) (PPA) derivative. The absorption and emission spectral characteristics of the polymer are discussed. Analogous to PPA, a subsequent thermal process leads to a cyclic trimer. Differential scanning calorimetry of EBA exhibits at least four exothermic processes, and these are discussed in terms of the polymerization and subsequent processes that ultimately lead to the cyclotrimer.

Introduction

The solid-state polymerization of diacetylenes[1−6] leads to conjugated polydiacetylenes (PDA), available as macroscopic polymer single crystals in optimal cases. While PDA crystals provide useful materials for the study of third-order nonlinear optical phenomena and electronic carrier mobility,[1,2,4,5] they exhibit an extremely low quantum yield for fluorescence.[7] If one wished to study fluorescence and related phenomena in a conjugated polymer single crystal, new solid-state reactions would have to be developed. It is in this context, and ultimately toward this end, that we initiated a study of the solid-state thermal reactivity of *p*-ethynylbenzoic acid (EBA).

It was earlier suggested[8] that the color change that occurred upon heating solid EBA was a slow solid-state polymerization. However, the structural basis for this possibility was not available.[8,9] In the absence of structural information, it is conceivable that, in addition to a polymerization, the solid-state reaction might involve a solid-state Strauss reaction[10] or a cyclotrimerization.[11] The work presented here, a study of the crystal structure of EBA as well as characterization of the product of the thermal reaction as a polymer, establishes the structure of the product and indicates the nature of the initiation of the thermal process. While exposure of EBA to ^{60}Co γ radiation (500 kGy) and UV light did not lead to a preparatively useful reaction, we found that the thermal reaction of crystalline EBA yields amorphous poly((4-carboxyphenyl) acetylene) (PCPA) when heated at temperatures <120 °C. When heated at temperatures >120 °C, the product is a mixture (Scheme 1) of PCPA and the cyclotrimer 1,3,5-tris(4-carboxyphenyl)benzene (TCPB). Furthermore, the TCPB component is a consequence of the thermal degradation of the PCPA backbone, similar to the thermal decomposition of solid poly(phenylacetylene) (PPA) at temperatures >120 °C.[12]

* Authors to whom correspondence should be addressed. E-mail: Daniel_Sandman@uml.edu (D.J.S.); foxman1@brandeis.edu (B.M.F.).

Scheme 1

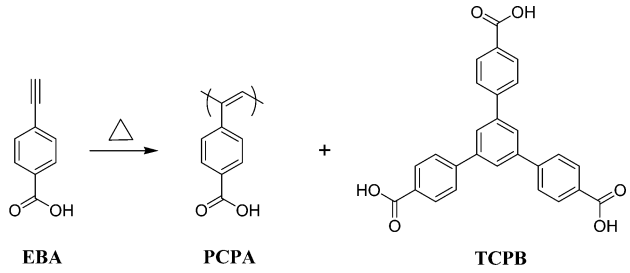

We decided to investigate the reactivity of a monoacetylene such as EBA as an extension of our earlier studies of approaches to solid-state polymerizations of a variety of crystalline acetylenes. Despite short intermolecular contacts between acetylenic groups, 10-undecynamide[13] is unreactive to heat, UV light, and ionizing radiation, and the observed reactivity of the semicarbazone of propiolic aldehyde[14] to γ irradiation is traceable to the presence of chlorinated solvents in crystal defects. Metal propynoates react[15−22] upon γ irradiation to produce polypropynoates in a crystalline monomer to amorphous polymer transition. Hence, the presence of both alkyne and carboxyl groups in EBA made it attractive to study. The alkali metal salts of EBA were reported[8] to be unreactive.

EBA is also an aryl acetylene. There are other reported examples of aryl acetylenes that polymerize in the solid state. The thermal and photochemical treatment of crystalline 1,4-diethynylnaphthalene[23−25] and 2,3-dichloro-1,4-diethynylnaphthalene,[25] the γ irradiation of crystalline 1,4-diethynylbenzene,[26] 3-[2-(3-acetoxy-1-propynyl)-4,5-dimethylphenyl]-2-propynyl acetate,[26,27] and 3-[4-(3-acetoxy-1-propynyl)-2,5-dimethylphenyl]-2-propynyl acetate[26,27] all result in amorphous products with polyene structures. Several crystalline di-*p*-ethynylbenzoyl ester compounds[28] and *N*,*N*′-bis(4-ethynylphenyl)-1,4,5,8-naphthalimide[29] thermally polymerize to give highly cross-linked polyene structures.

10.1021/ma0508451 CCC: $30.25
Published on Web 08/12/2005

Scheme 2

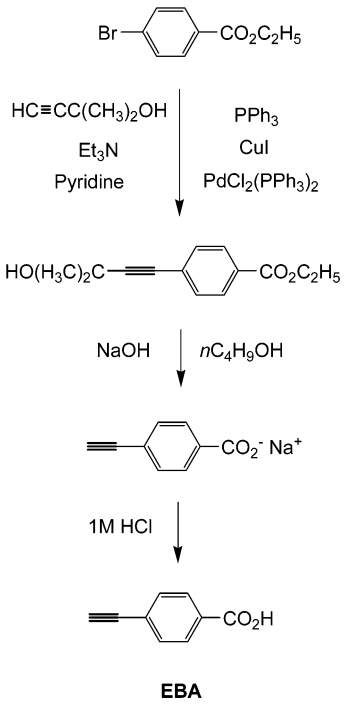

EBA

Experimental Section

Materials. All chemicals and solvents were purchased from Aldrich Chemical Co., and deuterated solvents were purchased from Cambridge Isotopes Lab.

Instrumentation. ^{1}H and ^{13}C NMR spectra were obtained utilizing a 500 MHz Bruker Avance DRX spectrometer. The chemical shifts of solvents CD_3OD and DMF-d_7 were internally referenced to TMS ($\delta = 0$ ppm), and the ^{13}C NMR spectra were recorded with proton decoupling. Infrared (IR) spectra were measured on a Perkin-Elmer Spectrum One-FTIR spectrometer. UV−vis spectra were recorded on a Perkin-Elmer UV/VIS/NIR Lambda 9 spectrometer. Fluorescence spectra were measured on a SLM 8000C spectrometer. Differential scanning calorimetry (DSC) scans were recorded in sealed pans under N_2 atmosphere with a DSC 2910 TA instrument. Molecular weights were measured by gel permeation chromatography (GPC) with a Waters HPLC system equipped with a model 510 HPLC pump, model 410 differential refractometer, model 441 absorbance detector, on-line multiangle laser light scattering (MALLS) detector (MiniDawn, Wyatt Technology Inc.), Model 712 sample processor, and five Ultrastyragel GPC columns connected in the following series: 500, 10^3, 10^4, 10^5, and 100 Å. The molecular weights were calculated with the Astra 1.4 program using a 100% recovery method. The carrier solvent was THF with a flow rate of 1 mL/min.

Synthesis of EBA. EBA was prepared utilizing a slightly modified synthetic route (Scheme 2) developed by Melissaris and Litt.[8] Ethyl *p*-bromobenzoate (64.5 g, 0.28 mol) was coupled to 2-methyl-3-butyn-2-ol (28.21 g, 0.34 mol) using a $PdCl_2(PPh_3)_2$ (0.23 g, 0.00033 mol) catalyst in a solution of anhydrous pyridine (160 mL), triethylamine (390 mL), cuprous iodide (0.22 g, 0.0011 mol), and triphenylphosphine (0.84 g, 0.0032 mol). The reaction was carried out in a dry 1-L round-bottom flask containing a magnetic stir bar and fitted with a water-cooled condenser. The solution was refluxed under argon for 2 h. The mixture was cooled to room temperature, filtered to remove the insoluble triethylamine hydrobromide, and the salt washed with triethylamine and diethyl ether until the ether washings were clear. The combined filtrates were reduced under vacuum to a solid material. The solid was then rinsed with water, purified with Soxhlet extraction using toluene, and dried under vacuum. The resulting ester was hydrolyzed and deprotected with NaOH (4 equiv) in *n*-butanol (600 mL) after 4 h at reflux to give the sodium salt of EBA, isolated by suction filtration. Acidification of an EBA-Na/water solution with 1 M HCl liberated the acid, yielding 18.0 g (44%) EBA. The monomer was recrystallized from toluene, yielding a light-tan, microcrystalline powder. The EBA powder darkened in color when stored at room temperature.[8,9,30] IR (KBr, cm^{-1}): 3270 (≡CH), 2670 and 2555 (CO_2H), 1685 (C═O). ^{1}H NMR (δ ppm, DMF-d_7): 4.41 (s) (1H, ethynyl), 7.67 (d) (2H, aromatic, $J = 8.2$ Hz), 8.04 (d) (2H, aromatic, $J = 8.2$ Hz), 13.53 (br) (1H, CO_2H). ^{13}C NMR (δ ppm, DMF-d_7): 82.72 and 83.10 (ethynyl), 126.78, 129.93, 131.62, and 132.37 (aromatic), 167.06 (CO_2H). Melting point 220−223 °C (dec). (lit.[8] mp 224−225 °C dec, lit.[9] mp 204−210 °C dec, lit.[30] mp 220−223 °C dec, lit.[31] mp 222−223 °C dec)

Table 1. Crystallographic Data for EBA

compound	EBA
chemical formula	$C_9H_6O_2$
a, Å	3.8684(4)
b, Å	6.2329(4)
c, Å	30.190(3)
α, deg	90
β, deg	90.281(8)
γ, deg	90
V, Å^3	727.91(11)
Z	4
formula wt, g/mol	146.15
space group	$P2_1/n$
T, °C	294 k
λ, Å	0.71073
ρ_{calc}, g cm^{-3}	1.333
μ, cm^{-1}	0.095
transmission factors	0.96−1.00
R^a	0.0402
$R_w{}^b$	0.0470
S^c	1.1567
no. reflections	569
no. parameters	100

[a] $R = \sum ||F_o| - |F_c||/\sum |F_o|$. [b] $R_w = [\sum_w(|F_o| - |F_c|)^2/\sum_w|F_o|^2]^{1/2}$. [c] $S = [\sum_w(|F_o| - |F_c|)^2/(n - m)]^{1/2}$.

X-ray Structure Determination of EBA. Single crystals of EBA were obtained from a warm toluene solution. A single crystal of EBA was selected and mounted on a Pyrex fiber affixed to a brass pin. The crystal was optically centered and placed on an Enraf-Nonius CAD4-Turbo diffractometer. X-ray data were collected using the Enraf-Nonius EXPRESS[32] program. The structure of EBA was solved by direct methods using SIR-92 and refined using the Oxford CRYSTALS package.[33] Nonhydrogen atoms were refined using anisotropic displacement parameters. The acidic hydrogen atom was located by difference map; all hydrogen atoms were placed at calculated positions ($d_{C-H} = 0.95$ Å; $d_{O-H} = 0.82$ Å). All hydrogen atoms were held fixed during the refinement and updated after each least-squares cycle. Complete crystallographic data is presented in Table 1. X-ray powder diffraction of EBA yielded the following single-phase pattern (*d* spacings (Å) > 3.00, s = strong reflection): 16.35, 15.77, 15.07 (s), 7.55, 5.27, 4.82, 4.34, 3.61, 3.25 (s), 3.21, and 3.12.

Isothermal Heating Products of EBA (A, B). Powdered crystals of EBA (200 mg) were placed in a 100-mL round-bottom flask and heated in an oil bath at 115 °C (**A**), and at 125 °C (**B**), under N_2 for 3 days. The dark reddish-brown colored products were then extracted for 3 days in a Soxhlet extractor using toluene to remove the unreacted monomer. The products were vacuum dried at ~60 °C for 7−10 days yielding (**A**: 34%, **B**: 42%) red (**A**) and orange (**B**) powders entirely free of monomer and toluene. The products are soluble in DMF, CH_3OH, and DMSO, partially soluble in THF, and insoluble in toluene. NMR and GPC analysis of the thermal products indicated that **A** consisted of pure PCPA, whereas **B** consisted of a near-equal mixture of TCPB and PCPA (see text). The thermal products were found to be amorphous by X-ray powder diffraction.

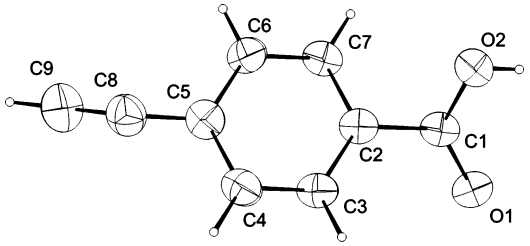

Figure 1. Molecular Structure of EBA, showing 50% probability ellipsoids for atoms refined by using anisotropic displacement parameters.

A: IR (KBr, cm^{-1}): 2640 and 2525 (CO_2H), 1690 (C=O). ^1H NMR (δ ppm, CD_3OD): 5.7−8.3 (br, CO_2H, aromatic, and vinyl). ^{13}C NMR (δ ppm, CD_3OD): 125−148 (br, aromatic and vinyl), 168−170 (br, CO_2H). UV−vis (DMF, ϵ/per unit): λ_{max} at 283 nm (6000) and tails out past 500 nm. Fluorescence (C = 0.69 mmol sol in DMF): (λ_{exc} = 350 nm), λ_{max} at 435 nm; (λ_{exc} = 400 nm), λ_{max} at 443 nm.

B: IR (KBr, cm^{-1}): 2645 and 2535 (CO_2H), 1690 (C=O). ^1H and ^{13}C NMR shifts of PCPA component in **B** are similar to **A**. ^{13}C NMR, TCPB component in **B** (labeled below) (δ ppm, CD_3OD): 169.77 (C1), 146.36 (C5), 142.97 (C6), 131.53 (C3), 130.74 (C2), 128.45 (C4), and 126.99 (C7).

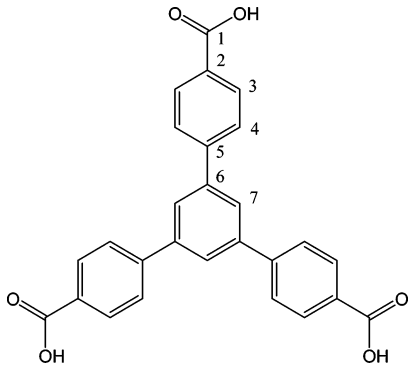

Thermal Product Obtained from DSC Scans of EBA (C). Good quality EBA crystals were thermally reacted by performing DSC scans (sealed aluminum pans) on three different samples at three different rates (see text) from 30 to 250 °C; the weight of each sample ranged from 5 to 6 mg. The three sample pans were then opened and combined as a single product (**C**), a reddish reflective material (100% yield). The melting transition, NMR, and GPC analysis (see text) of **C** indicated that the product was a mixture of TCPB (~90%) and PCPA (~10%).

C: IR (KBr, cm^{-1}): 2665 and 2550 (CO_2H), 1690 (C=O). ^1H NMR, TCPB component (δ ppm, DMF-d_7): 13.16 (s) (CO_2H), 8.24 (s) (central ring), 8.20 (d) (*meta*-H of 1,3,5-rings, J = 8.2 Hz), 8.17 (d) (*ortho*-H of 1,3,5-rings, J = 8.2 Hz). ^{13}C NMR, TCPB component (δ ppm, DMF-d_7): 167.58 (C1), 144.72 (C5), 141.61 (C6), 130.40 (C3), 129.89 (C2), 127.85 (C4), and 126.19 (C7). Melting point 305−310 °C (dec). (TCPB; lit.[34] mp 315−318 °C, lit.[35] mp 325 °C).

Results and Discussion

Crystal Structure of EBA. The molecular structure and numbering scheme for EBA is shown in Figure 1; bond lengths and angles lie in normal ranges. Several molecular packing features are obvious from the crystal structure of EBA (Figure 1). Figure 2 shows the packing of EBA down the a-axis; hydrogen bonding of the carboxylate group [O2···O1(3-x, −1-y, 2-z)] exhibits the common dimeric $\mathbf{R_2^2(8)}$ graph set pattern. Further, there is a weak C−H···π interaction [C9−H91···C8/C9$_{midpoint}$(3/2-x, y-1/2, 3/2-z), 3.74 Å C···C, 2.74 Å H···C, C−H···π, 170.2°] that forms "T-shaped caps" at each end of the carboxylate dimer. The C−H···π patterns observed here are similar to the characteristic hydrogen bonding patterns in many other terminal alkyne compounds.[23,36−38]

Extensive π···π interactions between the aromatic rings leads to a short crystallographic axis, a = 3.87 Å, with carboxylate dimer pairs stacked at an angle of 25.8° to the a-axis. The shortest α···β' intermolecular contact, between parallel acetylene moieties (contact "a" in Figure 3), occurs along the a direction: 3.71 Å [C9···C8(x-1, y, z)]. A second short interaction, 3.82 Å [C9···C8(3/2-x, y-1/2, 3/2-z)], between nearly perpendicular acetylene moieties and coincident with the putative C−H···π interaction, is shown as contact "b" in Figure 3.

Characterization of Thermal Products. The GPC results of products **A**−**C**, obtained from the thermal reaction of crystalline EBA (see Experimental Section), are given in Figure 4. The molecular weight (M_n) distribution profiles of **B** and **C** are characteristically

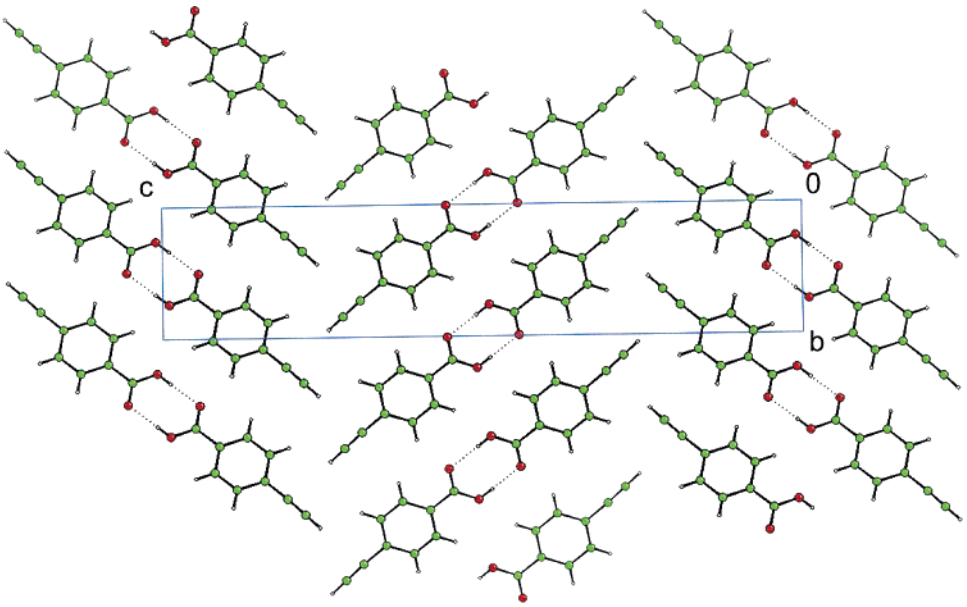

Figure 2. Crystal structure of EBA viewed along the a-axis.

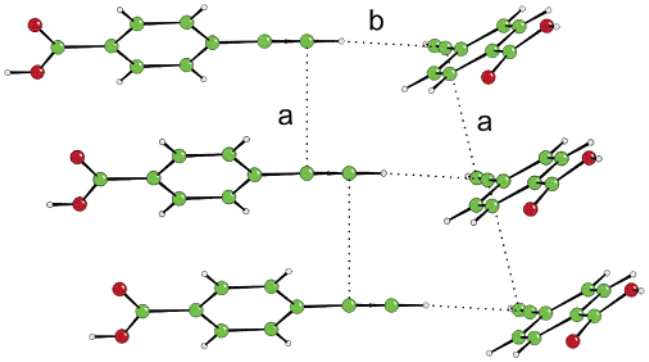

Figure 3. Short α···β′ C≡C···C≡C intermolecular contacts (a = 3.71, b = 3.82 Å).

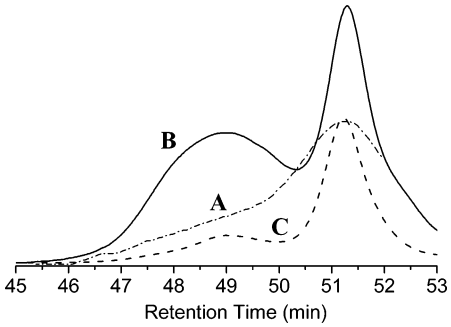

Figure 4. GPC analysis of A (dash−dot), B (solid), and C (dash). A−C: distribution maximum at ∼51.3 min signifies M_n ∼ 400 g/mol. B−C: the distribution maximum at ∼49 min signifies M_n ∼ 2000 g/mol.

similar, and consist of bimodal M_n distributions with peaks at ∼400 and ∼2000 g/mol. On the basis of the NMR spectra (vide infra) of **B** and **C**, the former peak likely represents the cyclic trimer, TCPB, and the latter peak represents oligomeric PCPA. Because the two overlapping distributions are symmetrical, it is unlikely that aggregation of the two species significantly alters the peak M_n values. Thus, the maximum size of PCPA in **B** and **C** is about 13 units. By comparing the relative areas of the two distribution curves, the GPC data suggests the ratio of TCPB to PCPA in products **B** and **C** is ∼1:1 and ∼10:1, respectively. Unlike these products, the profile of **A** consists of a single, relatively broader M_n distribution at ∼400 g/mol, and a descending tail in the region near ∼2000 g/mol. The NMR spectra of **A** indicate that the product is pure PCPA, which suggests that the peak at ∼400 g/mol is likely the linear trimer of EBA, and the continuous tail represents a distribution of PCPA with a range of about 4−13 units.

A plethora of studies used IR[12,39−43] and/or NMR[12,41−50] spectroscopy to examine the assorted stereostructures of PPA. The IR measurements were obtained from the fingerprint (∼1400−700 cm^{-1}) region of PPA, and because this region changes considerably upon para-substitution of the aromatic ring, IR data of PPA was inapplicable to stereostructural analysis of several functional derivatives of PPA.[51] Conversely, NMR has been demonstrated to be a useful technique for characterizing the stereostructures of a variety of para-substituted PPA derivatives,[51−54] such as regioregular *cis*-PCPA.[55−57] In fact, the NMR spectra of regioregular *cis*-PPA[46] and *cis*-PCPA[57] are nearly identical. Furthermore, the relative cis content is available from ^{1}H NMR measurements of cis-rich PPA. The ^{1}H NMR spectra of PPA materials consisting of a stereoregular cis content of about 70% or greater display sharp, well-resolved peaks, whereas the spectra of regiorandom polymers are broad and featureless.[12,43]

The IR, ^{1}H, and ^{13}C NMR spectra of products **A**−**C** clearly indicated that the ethynyl group had been entirely consumed in the solid-state reaction; however, the IR spectra were nearly identical. Therefore, only the NMR spectra were capable of distinguishing between the PCPA and TCPB components and stereostructural examination of PCPA. The ^{13}C NMR spectrum of **A** (Figure 5, upper) displays, for the most part, broad and unresolved chemical shifts. The resonances between ∼125−132 ppm represent the tertiary (=CRH) aromatic and alkene carbons of PCPA, and the range from ∼135−148 ppm, though barely distinguishable from the baseline, represents the (=CR_2) quaternary carbons of PCPA. This resonances between ∼168−170 ppm represent the CO_2H carbons. The broad =CRH and near-featureless =CR_2 resonances of **A** closely resemble the ^{13}C NMR spectra of regiorandom PPA[41,44,46] and poly(methyl *p*-ethynylbenzoate).[52] However, the spectrum does consist of a few sharp peaks atop the broad distribution from ∼125−132 ppm; the most notable peak is at 130.84 ppm. These relatively sharp peaks may represent the aromatic =CRH shifts of the smaller (i.e., trimer/tetramer) PCPA species. Likewise, the ^{1}H NMR spectrum of **A** consists of a single broad peak ranging from ∼5.7−8.3 ppm and is analogous to the ^{1}H NMR spectra of regiorandom PPA.[45−47]

Similar to **A**, the ^{13}C NMR spectra of thermal products **B** and **C** display broad chemical shifts corresponding to atactic/*trans* PCPA. However, unlike **A**, the spectra also contain sharp, characteristic peaks of the TCPB component (Figure 5, middle/lower), which are consistent with the ^{13}C NMR shifts of TCPB,[58] 1,3,5-triphenylbenzene,[41,50] and a strikingly similar compound, 4,4″-dicarboxy-5′-phenyl-*m*-terphenyl.[59] In fact, the relative amounts of PCPA and TCPB in **C** and **B** are noticeable from comparison of ^{13}C signal intensities of the TCPB and PCPA components in the chemical shift range of ∼125−132 ppm. In this range, the intensities of the PCPA and TCPB shifts are approximately the same for product **B**, and like the GPC analysis, suggest an equal concentration of each component. On the other hand, the intensities of the TCPB shifts in **C** are considerably greater than the PCPA resonances, which indicates that the product is predominately TCPB, consistent with the GPC and melting transition of **C**. Further evidence for the abundance of TCPB in **C** is available from the ^{1}H NMR spectrum (Figure 6). Because approximately half of **B** is PCPA, the interpretation of the ^{1}H shifts representing the TCPB component is complicated by overlap with the broad PCPA resonances. However, because **C** is primarily TCPB, the relatively unobscured spectrum displays a chemical shift pattern similar to the aromatic region of pure TCPB,[58] which consists of a downfield singlet for the protons of the central ring and the typical coupling pattern of two, closely spaced, chemical shifts representing the ortho and meta protons of the 1,3,5-rings.

Last, it is worth mentioning that the ^{13}C spectra of products **A**−**C** did not contain shifts in the ∼50−70 ppm range. Peaks in this range have been identified by Percec et al. as cyclohexadiene defect structures.[44] Thus, it is unlikely that **A**, and the PCPA component in products **B** and **C**, contain cyclohexadiene sequences.

Optical Measurements of PCPA. The UV−vis absorption and fluorescence emission spectra of oligo-

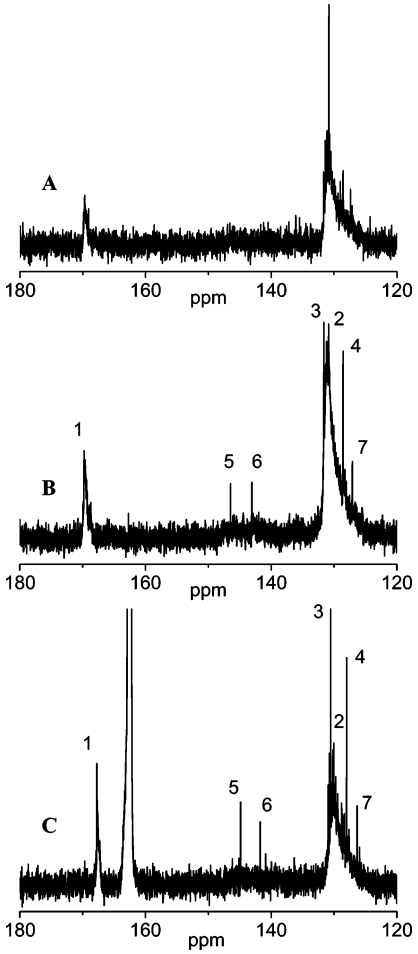

Figure 5. ^{13}C NMR spectra of thermal products A (upper, in CD_3OD), B (middle, in CD_3OD), and C (lower, in DMF-d_7). The large peak at 163.15 ppm in the spectrum of C is from DMF-d_7. The labeled peaks denote the TCPB component (see Experimental Section); NMR shifts of TCPB according to literature.[59] Each spectrum represents 25 k scans.

meric PCPA (**A**) in DMF and methanol solutions are shown in Figure 7. On the basis of electronic spectroscopy studies of PPA, the absorption of PCPA at wavelengths longer than 250 nm is due to $\pi-\pi^*$ interband transitions of the polyacetylene backbone.[45,47,61] Furthermore, this relatively featureless tail from ~300−500 nm is similar to the absorption spectra of regiorandom PPA.[40,45] Like NMR, UV−vis spectroscopy is sensitive to the regioregular segments of the polyacetylene chain. Stereoregular PPA consisting of a cis content greater than ~80% displays two absorption maxima at ~330 nm and ~400 nm.[45,47,62] Additionally, complexation with chiral amines induces circular dichroism in stereoregular *cis*-PCPA.[55−57]

PPA also exhibits fluorescence.[40,47,61,63,64] Although discrepancies exist in the literature, the emission maximum of regiorandom PPA generally occurs at ~420−430 nm.[40,61,63] Likewise, **A** exhibits a broad fluorescence, with peaks centered at 435 and 443 nm, respectively, when excited with wavelengths of 350 and 400 nm. The corresponding variation in the emission peak with excitation wavelength is a consequence of a broad M_n distribution.[63]

Thermal Analysis of EBA and PCPA. The yields of **A** and **B** (34 and 42%, respectively) are relatively low because of competition with sublimation in the flasks under a nitrogen atmosphere. Sublimation under these

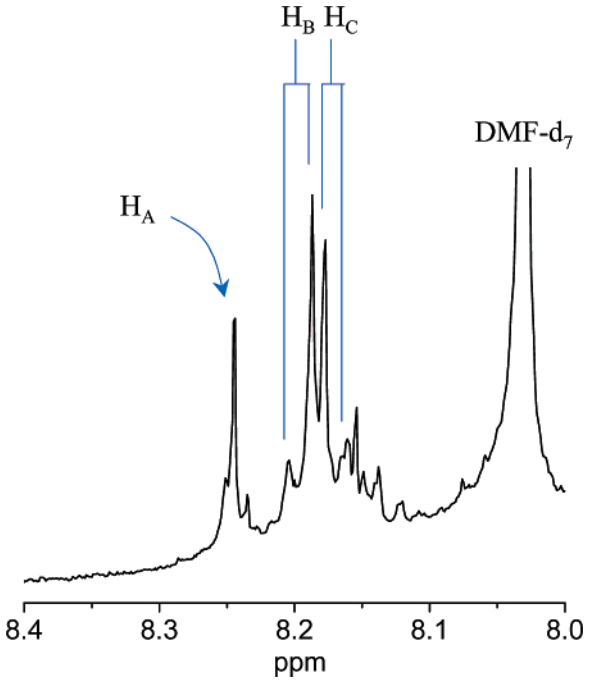

Figure 6. ^1H NMR spectrum of C in DMF-d_7, displaying the aromatic region of the TCPB protons. H_A is the proton of the central ring. H_B and H_C are the meta and ortho protons, respectively, of the outer 1,3,5 rings with $J = 8.2$ Hz. Chemical shift assignments according to literature[58] and theoretical shift calculations using ACD software.[60]

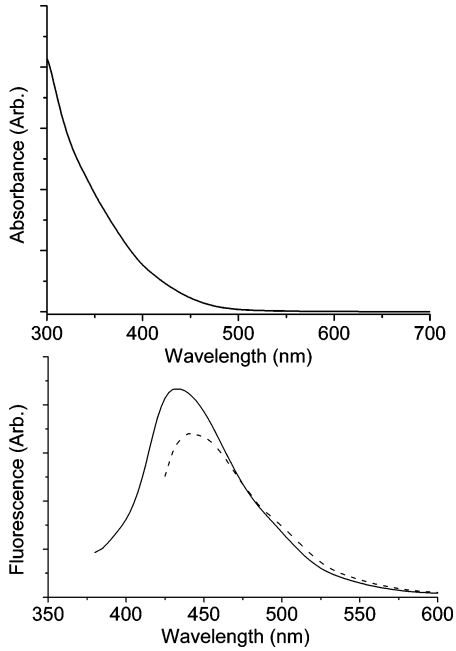

Figure 7. UV−vis absorption (upper) and fluorescence emission (lower) spectra of A in DMF solutions. Excitation wavelengths: 350 nm (solid line), 400 nm (dotted line).

conditions is common for benzoic and cinnamic acid derivatives. The DSC thermogram of PCPA, obtained at 5 °C/min, is displayed in Figure 8. The scan consists of a small exothermic peak at 85 °C, which transforms into small endothermic dip, and a large exothermic peak at 177 °C. It is unclear as to what causes the former, consecutive, exo- and endothermic transitions, but rationale for the latter, larger exothermic transition is available from thermal studies of PPA.

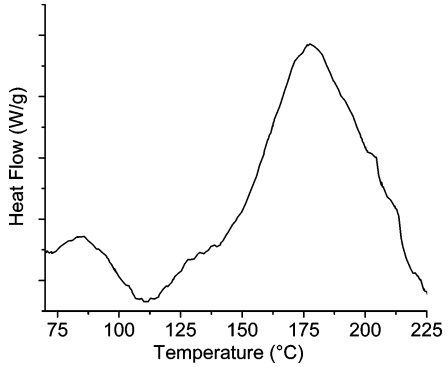

Figure 8. DSC thermogram of A with a scan rate of 5 °C/min.

DSC scans of regiorandom PPA[65] resulted in a single exothermic peak near ~200 °C, whereas DSC scans of regioregular *cis*-PPA,[66] and a para-substituted *cis*-PPA derivative,[54] displayed two transitions near ~170 and ~200 °C. The two exothermic transitions of *cis*-PPA represent cis−trans isomerization and chain cyclization/scission processes, respectively, whereas the single transition of regiorandom PPA represents both isomerization and cyclization/scission processes. Regardless of the stereostructure, the primary thermal cyclization/scission products of PPA are triphenylbenzene compounds.[67] Thus, it is possible that the broad exothermic transition peaked at 177 °C represents isomerization and chain cyclization/scission processes, analogous to the single exothermic transition of regiorandom PPA.

Interestingly, DSC scans of three crystalline EBA samples (Figure 9) resulted in a series of four exothermic transitions between 181 and 221 °C, when heated anywhere from 2 to 10 °C/min. Specifically, a scan rate of 2 °C/min (Figure 9, upper) resulted in exothermic transitions with peaks at 181, 190, 196, and 200 °C; a scan rate of 5 °C/min (Figure 9, middle) resulted in peaks at 193, 203, 208, and 211 °C; and a scan rate of 10 °C/min (Figure 9, lower) resulted in peaks at 201, 210, 218, and 221 °C. Furthermore, a second DSC scan at 10 °C/min (Figure 9, lower) did not display a single thermal transition, and resulted in a flat line out to 250 °C. NMR analysis of the DSC products indicated that the samples had undergone 100% conversion in the first scan, and that the collective product (**C**) is predominantly TCPB (*vide post*). The absence of any thermal transitions below 250 °C is because TCPB melts at temperatures greater than 300 °C.[34,35]

The exothermic transitions suggest that at least four processes are involved in the transformation of crystalline EBA to amorphous TCPB. While we contemplated the idea of the first two exothermic peaks as possible addition steps, such as dimerization and trimerization, information pertaining to the isothermal products (**A**−**B**) and polymerization studies of phenylacetylene suggested a different scenario. The isothermal treatment of phenylacetylene at temperatures greater than 140 °C results, primarily, in oligomeric PPA, and a relatively small amount of 1,3,5-triphenylbenzene.[12,39] Similarly, the major product from the isothermal treatment of EBA at 115 °C (**A**) is the linear trimer of PCPA (**A**), whereas treatment at 125 °C (**B**) gives oligomeric PCPA and TCPB. The lone formation of 1,3,5-cyclotrimers indicates that only head-to-tail type bonds take place in thermal reactions of phenylacetylene and EBA.[45,54,67] However, the symmetrical cyclotrimer is the smallest head-to-tail product of phenylacetylene, as the (head-to-tail) dimer product has not been isolated, regardless of the polymerization method.[12,39,41,42,50,68] The propensity of EBA, and phenylacetylene, to form trimer-sized species suggests that the initial solid-state product is the linear trimer of PCPA. Therefore, the first exothermic transition is likely the formation of oligomeric PCPA, and the latter three exothermic transitions are relevant to the formation of TCPB via cyclization/chain scission processes of PCPA. One plausible scenario is that upon polymerization (first exotherm), oligomeric PCPA subsequently undergoes isomerization (second exotherm), cyclization (third exotherm), and chain scission (fourth exotherm). While the actual mechanisms of the latter three exotherms are not understood at this time, they likely concern isomerization, cyclization, and chain scission mechanisms, similar to the exothermic transitions of cis-rich PPA.[45,66,69]

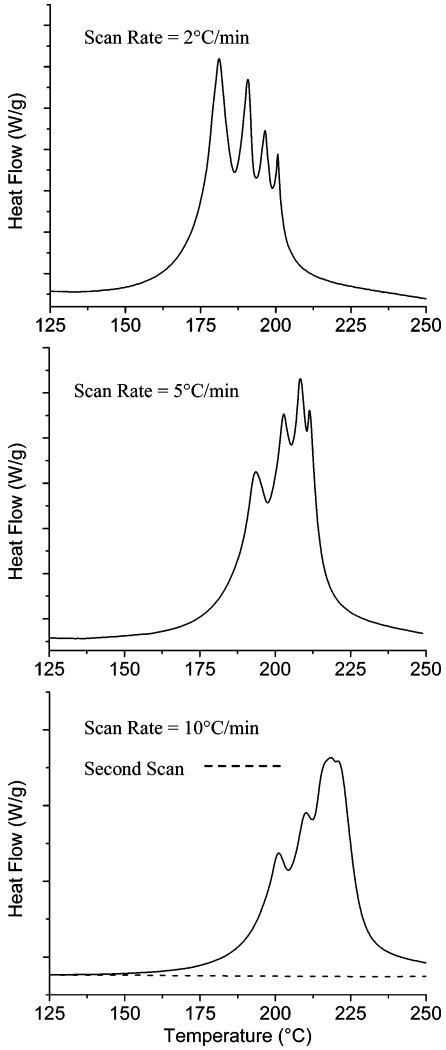

Figure 9. DSC scans of three crystalline EBA samples with different heating rates; the collective product of which is C. Upper: 2 °C/min. Middle: 5 °C/min. Lower: 10 °C/min; dotted line represents a second scan of this sample.

Structure and Reactivity of Crystalline EBA. Recrystallization of EBA from toluene at room temperature resulted in orange crystals (Figure 10); the orange color develops over several days. The orange color is due to initiation of polymerization of solid EBA at room temperature.[8,9] The EBA crystals turn red when heated at temperatures greater than ~80 °C. Similarly, UV irradiation (λ_{exc} = 254 nm) of the crystalline monomer

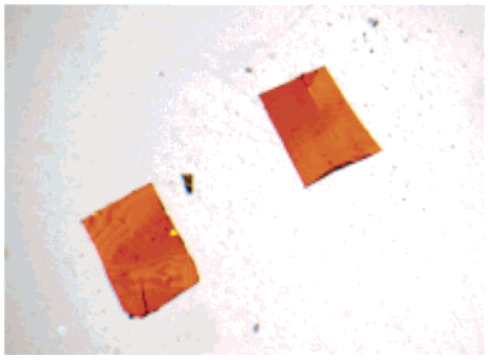

Figure 10. Photograph of two EBA crystals. The crystals are ~0.3 mm^2 in dimension, and ~0.1 mm thick.

results in a dark-red material in only a few hours. However, the irradiated crystals contain only trace amounts of product, which may indicate that absorption occurs predominantly at the surface. Despite the low yields, this photochemically induced reaction of EBA may suggest that the initiation of the polymerization is topochemical, similar to solid-state initiation of various diacetylenes[70] and cinnamic acids.[71−73]

The fundamental assumption associated with a topochemical process is the principle of least motion, meaning the motions of the monomer molecules through the course of the reaction are at an absolute minimum.[74] Consequently, because the crystalline lattice influences the directionality of molecular motion, the conformation of the initial product resembles the relative orientation (molecular packing) of the particular molecules prior to reaction.[72] However, regardless of the types of motions involved in topochemical reactions, the adjacent molecules must be close enough to one other for a reaction to take place. In fact, comprehensive studies of *trans*-cinnamic acids[72] and diacetylenes[75] revealed that reactivity primarily occurs in crystals consisting of interatomic distances of about 4.2 Å, or less, between the participating functional groups. While other crystallographic factors may be relevant to the topochemical reactivity of a particular class of materials, such as the angle[75] between the diacetylene rod and the stacking axis, it is the criterion of 4.2 Å that appears to be significant to the vast majority of reactive crystal structures.

While the criteria for topochemical reactivity has been established for a wide variety of diacetylenes and *trans*-cinnamic acids, the structural criteria, if any, for reactivity of crystalline terminal alkyne compounds has not been fully examined. The majority of information regarding both structure−reactivity relationships for terminal alkynes is available from ^{60}Co γ irradiation studies of various metal propynoates (MPs)[15−21] and 1,4-diethynylbenzene (DEB)[26] and UV and thermal polymerization studies of 1,4-diethynylnaphthalene (DEN).[23−25] The solid-state polymerization of crystalline EBA, DEN, DEB, and (reactive) MPs results in amorphous polyene materials. X-ray diffraction studies of heated single crystals of EBA showed either only weaker diffraction from the monomer lattice, or a total loss of crystallinity, consistent with the formation of amorphous product. The crystal structures of EBA (Figure 3), DEN,[23] DEB,[37,38] and reactive MPs[15−21] all contain sets of infinite, linear arrays of alkyne groups with intermolecular distances of less than 4.2 Å between adjacent alkyne carbon atoms; for UV- or radiation-induced (X- or γ-rays) reactions, this appears to be a simple, valid criterion that may readily be used both to predict and rationalize the onset of reactivity. Topochemical criteria for thermal reactivity are considerably less well-understood; large separations do not necessarily preclude solid-state reactivity.[76,77] Nonetheless, it is apparent that topochemical effects play a role in the initiation step for thermal reactions in the solid state. The conditions under which a given reaction affords a topochemical product, with fine stereochemical control throughout the process, remain poorly defined.[78]

Because the thermal degradation product (TCPB) of PCPA is a symmetrical cyclotrimer, the PCPA backbone must arise from a head-to-tail addition.[45,54,67] Thus, upon initiation, a head-to-tail addition could occur via translational diffusion of the EBA molecules along the *a*-axis. Furthermore, because the relative distance between the reactive PCPA chain ends and closest EBA monomer molecules (along the *a*-axis) increases[73] with propagation, phase separation (termination) likely occurs as the PCPA chains separate from the monomer matrix, resulting in oligomeric PCPA.

Conclusions.

The linear chain crystal structure of EBA reported herein with its short intermolecular contacts provides a structural basis for the observed[8] color change and subsequent initiation of topochemical thermal solid-state polymerization. With respect to phenylacetylene, the thermal solid-state polymerization of EBA is relatively easier to control. The thermal treatment of crystalline EBA results in oligomeric PCPA when isothermally heated at temperatures less than ~120 °C, whereas rapid heating of EBA to ~250 °C results in the predominant formation of TCPB via cyclization of PCPA. To our knowledge, there are no thermal polymerization studies of phenylacetylene leading to PPA, or 1,3,5-triphenylbenzene, as the sole product. Because phenylacetylene is a liquid at room temperature, the ability to isothermally manipulate the reaction product of EBA, via a topochemical thermal initiation, is likely due to the influence of the crystal structure.

Acknowledgment. The work at the University of Massachusetts Lowell was supported in part by the Petroleum Research Fund Grant 40263-AC7. The work at Brandeis University was supported in part by the National Science Foundation through grant DMR-0504000. The authors thank Dr. Laszlo Sipos for the GPC analysis and M. J. Downey for furnishing the X-ray powder data.

Supporting Information Available: Crystallographic information file (as PDF) for EBA. This material is available free of charge via the Internet at http://pubs.acs.org.

References and Notes

(1) Bloor, D., Chance, R. R., Eds. *Polydiacetylenes*; Martinus Nijhoff, NATO ASI Series; Dordrecht: Boston, 1985.
(2) Sandman, D. J., Ed. *Crystallographically Ordered Polymers*; ACS Symposium Series 337; American Chemical Society: Washington, DC, 1987.
(3) Chance, R. R. In *Encyclopedia of Polymer Science and Engineering*, Kroschwitz, J. I., Ed.; Wiley-Interscience: New York, 1986; Vol. 4, pp 767−779.
(4) Pope, M.; Swenberg, C. E. *Electronic Processes in Organic Crystals and Polymers,* 2nd ed.; Oxford University Press: New York, 1999; pp 673−699; 809−824.
(5) Sandman, D. J. In *Polymeric Materials Encyclopedia*; Salamone, J. C., Ed.; CRC Press: Boca Raton, FL, 1996; Vol. 2, pp 1468−1480.

(6) Nakanishi, H. In *Polymeric Materials Encyclopedia*; Salamone, J. C., Ed.; CRC Press: Boca Raton, FL, 1996; pp 8398−8398.
(7) Sandman, D. J. *Trends Polym.Sci.* **1994**, *2*, 44−55.
(8) Melissaris, A. P.; Litt, M. H. *J. Org. Chem.* **1992**, *57*, 6998−6999.
(9) Ribera, G.; Galià, M.; Cádiz, V. *Macromol. Chem. Phys.* **2001**, *202*, 3363−3370.
(10) Cadiot, P.; Chodkiewicz, W. In *Chemistry of Acetylenes*; Viehe, H.-G., Ed.; Marcel Dekker: New York, 1969; pp 597−647.
(11) Swanson, S. A.; Fleming, W. W.; Hofer, D. C. *Macromolecules* **1992**, *25*, 582−588.
(12) Simionescu, C. I.: Percec, V.; Dumitrescu, S. *J. Polym. Sci., Polym. Chem. Ed.* **1977**, *15*, 2497.
(13) Sandman, D. J.; Velazquez, C. S.; Hamill, G. P.; Foxman, B. M.; Preses, J. M.; Weston, R. E., Jr. *Mol. Cryst. Liq. Cryst.* **1988**, *156*, 103−108.
(14) Sandman, D. J.; Hamill, G. P.; Samuelson, L. A.; Foxman, B. M. *Mol. Cryst. Liq. Cryst.* **1984**, *106*, 199−217.
(15) Foxman, B. M.; Jaufmann, J. D. *Mol. Cryst. Liq. Cryst.* **1984**, *106*, 187−197.
(16) Booth, C. A.; Foxman, B. M.; Jaufmann, J. D. In *Crystallographically Ordered Polymers*; Sandman, D. J., Ed.; ACS Symposium Series 337; American Chemical Society: Washington, DC, 1987; pp 99−105.
(17) Case, C. B.; Foxman, B. M. *Inorg. Chim. Acta* **1994**, *222*, 339.
(18) Moloney, M. J.; Foxman, B. M. *Inorg. Chim. Acta* **1995**, *229*, 323.
(19) Brodkin, J. S.; Foxman, B. M.; Clegg, W.; Cressey, J. T.; Harbron, D. R.; Hunt, P. A.; Straughan, B. P. *Chem. Mater.* **1996**, *8*, 242−247.
(20) Foxman, B. M.; Vela, M. J. *Trans. Am. Crystallogr. Assoc.* **1998**, *33*, 75−84.
(21) Jaufmann, J. D.; Case, C. B.; Sandor, R. B.; Foxman, B. M. *J. Solid State Chem.* **2000**, *152*, 99.
(22) Vela, M. J.; Foxman, B. M. *Cryst. Eng.* **2000**, *3*, 11−31.
(23) Enkelmann, V.; Rohde, O. *Acta Crystallogr.* **1977**, *B33*, 3531−3533.
(24) Rohde, O.; Wegner, G. *Makromol. Chem.* **1978**, *179*, 1999−2011.
(25) Rohde, O.; Wegner, G. *Makromol. Chem.* **1978**, *179*, 2013−2029.
(26) Hagihara, M.; Yamamoto, Y.; Takahashi, S.; Hayashi, K. *Radiat. Phys. Chem.* **1986**, *28*, 165−167.
(27) Kai, Y.; Yamamoto, A.; Xu, D.; Kasai, N.; Hagihara, M.; Yamamoto, Y.; Takahashi, S.; Hayashi, K. *Makromol. Chem.* **1987**, *188*, 3047−3059.
(28) Melissaris, A. P.; Litt, M. H. *Macromolecules* **1994**, *27*, 2675.
(29) Melissaris, A. P.; Litt, M. H. *Polymer* **1994**, *35*, 3305.
(30) Havens, S. J.; Hergenrother, P. M. *J. Polym. Sci., Polym. Chem. Ed.* **1984**, *22*, 3011.
(31) Hergenrother, P. M. *J. Polym. Sci., Polym. Chem. Ed.* **1982**, *20*, 3131.
(32) Straver, L. H. *CAD4-EXPRESS;* Enraf-Nonius: Delft, The Netherlands, 1992.
(33) (a) Altomare, A.; Cascarano, G.; Giacovazzo, C.; Guagliardi, A.; Burla, M. C.; Polidori, G.; Camalli, M. *J. Appl. Crystallogr.* **1994**, *27*, 435. (b) Betteridge, P. W.; Carruthers, J. R.; Cooper, R. I.; Prout, K.; Watkin, D. J. *J. Appl. Crystallogr.* **2003**, *36*, 1487. (c) Watkin, D. J.; Prout, C. K.; Pearce, L. J. *CAMERON*, Chemical Crystallography Laboratory, University of Oxford:, Oxford, U.K., 2002.
(34) Weber, E.; Hecker, M.; Koepp, E.; Orlia, W.; Czugler, M.; Csöregh, I. *J. Chem. Soc., Perkin Trans. 2* **1988**, 1251.
(35) Svirbely, W. J.; Weisberg, H. E. *J. Am. Chem. Soc.* **1959**, *81*, 257.
(36) Steiner, T. *J. Chem. Soc., Chem. Commun.* **1995**, 95.
(37) Weiss, H. C.; Blaser, D.; Boese, R.; Doughan, B. M.; Haley, M. M. *Chem. Commun.* **1997**, 1703.
(38) Robinson, J. M. A.; Kariuki, B. M.; Gough, R. J.; Harris, K. D. M.; Philp, D. *J. Solid State Chem.* **1997**, *134*, 203.
(39) Kern, R. J. *J. Polym. Sci., Part A-1* **1969**, *7*, 621.
(40) Masuda, T.; Sasaki, N.; Higashimura, T. *Macromolecules* **1975**, *8*, 717.
(41) Cianciusi, A. M.; Furlani, A.; Ginestra, A. L.; Russo, M. V.; Palyi, G.; Visi-Orosz, A. *Polymer* **1990**, *31*, 1569.
(42) Douglas, W. E.; Overend, A. S. *J. Organomet. Chem.* **1993**, *444*, C62−C64.
(43) Mastrorilli, P.; Nobile, C. F.; Rizzuti, A.; Suranna, G. P.; Acierno, D.; Amendola, E. *J. Mol. Catal. A: Chem.* **2002**, *178*, 35.
(44) Percec, V.; Rinaldi, P. L. *Polym. Bull.* **1983**, *9*, 548.
(45) Matsunami, S.; Watanabe, T.; Kamimura, H.; Kakuchi, T.; Ishii, F.; Tsuda, K. *Polymer* **1996**, *37*, 4853.
(46) Tang, B. Z.; Poon, W. H.; Leung, S. M.; Leung, W. H.; Peng, H. *Macromolecules* **1997**, *30*, 2209.
(47) Lee, C. W.; Wong, K. S.; Lam, W. Y.; Tang, B. Z. *Chem. Phys. Lett.* **1999**, *307*, 67.
(48) Ishii, F.; Matsunami, S.; Shibata, M.; Kakuchi, T. *J. Polym. Sci., Part B: Polym. Phys.* **1999**, *37*, 1657.
(49) Percec, V.; Rudick, J. G.; Nombel, P.; Buchowicz, W. *J. Polym. Sci., Part A: Polym. Chem.* **2002**, *40*, 3212.
(50) Marigo, M.; Marsich, N.; Farnetti, E. *J. Mol. Catal. A: Chem.* **2002**, *187*, 169.
(51) Iwamura, H.; McKelvey, R. D. *Macromolecules* **1988**, *21*, 3386.
(52) Le Moigne, J.; Hilberer, A.; Strazielle, C. *Macromolecules* **1992**, *25*, 6705.
(53) Ting, C. H.; Chen, J. T.; Hsu, C. S. *Macromolecules* **2002**, *35*, 1180.
(54) Kong, X.; Lam, J. W. Y.; Tang, B. Z. *Macromolecules* **1999**, *32*, 1722.
(55) Yashima, E.; Matsushima, T.; Okamoto, Y. *J. Am. Chem. Soc.* **1995**, *117*, 11596.
(56) Yashima, E.; Matsushima, T.; Okamoto, Y. *J. Am. Chem. Soc.* **1997**, *119*, 6345.
(57) Saito, M. A.; Maeda, K.; Onouchi, H.; Yashima, E. *Macromolecules* **2000**, *33*, 4616.
(58) Jutand, A.; Negri, S. *Eur. J. Org. Chem.* **1998**, 1811.
(59) Spiliopoulos, I. K.; Mikroyannidis, J. A. *Macromolecules* **1998**, *31*, 1236.
(60) *ACD/HNMR Predictor Software*, version 4.56; Advanced Chemistry Development Inc.: Toronto, Ontario, Canada, 2000.
(61) Yu, G.; Liu, Y.; Zhan, X.; Li, H.; Yang, M.; Zhu, D. *Thin Solid Films* **2000**, *363*, 126.
(62) Cametti, C.; Codastefano, P.; Amato, R. D.; Furlani, A.; Russo, M. V. *Synth. Met.* **2000**, *114*, 173.
(63) MacCallum, J. R.; Hoyle, C. E.; Guillet, J. E. *Macromolecules* **1980**, *13*, 1647.
(64) Wong, K. S.; Lee, C. W.; Tang, B. Z. *Synth. Met.* **1999**, *101*, 505.
(65) Luyt, A. S.; Vosloo, H. C. M.; Reading, M. *Thermochim. Acta* **1998**, *320*, 135.
(66) Matsunami, S.; Kakushi, T.; Ishii, F. *Macromolecules* **1997**, *30*, 1074.
(67) Duc, S.; Petit, A. *J. Anal. Appl. Pyrolysis* **1997**, *40−41*, 55.
(68) Matusiak, R.; Keller, A. *Polym. Bull.* **1999**, *43*, 199.
(69) Cukor, P.; Rubner, M. *J. Polym. Sci., Polym. Phys. Ed.* **1980**, *18*, 909.
(70) Bassler, H. *Adv. Polym. Sci.* **1984**, *63*, 1.
(71) Ramamurthy, V.; Venkatesan, K. *Chem. Rev.* **1987**, *87*, 433.
(72) Schmidt, G. M. J *J. Chem. Soc.* **1964**, 2014.
(73) Hirshfeld, F. L.; Schmidt, G. M. J. *J. Polym. Sci., Part A: Polym. Chem.* **1964**, *2*, 2181.
(74) Cohen, M. D.; Schmidt, G. M. J. *J. Chem. Soc.* **1964**, 1996.
(75) Enkelmann, V. *Adv. Polym. Sci.* **1984**, *63*, 91.
(76) Wheeler, K. A.; Foxman, B. M. *Chem. Mater.* **1994**, *6*, 1330.
(77) Cheng, K.; Foxman, B. M. *J. Am. Chem. Soc*. **1977**, *99*, 8102.
(78) Di, L.; Foxman, B. M. *Supramol. Chem.* **2001**, *13*, 163.

MA0508451